Analysis of Energy Storage Devices to Enhance Power System Oscillation Stability – Part II Simulation and Extension

W.J. Du , Z.Chen, H.F.Wang and Rod Dunn
Southeast University, Nanjing, CHINA; University of Bath, Bath, UK; and The Queen's University of Belfast, Belfast, UK

Abstract-This paper proposes a novel theoretical method in studying the capability of an energy storage system installed in a power system to enhance system oscillation stability. The proposed method is developed based on the well-know equal-area criterion and small-signal stability analysis. In the paper, some useful analytical conclusions are presented. Simulation results of an example power system installed with a Battery Energy Storage System (BESS) are given and the extension to more complicated case of multi-machine power systems is also discussed briefly. This is part II of the paper.

Keywords: -Energy Storage Systems (ESS), Battery Energy Storage Systems (BESS), power system oscillations, equal-area criterion

1 Demonstration of an example power system

An example power system of Figure 1 is constructed. The system parameters and initial operating condition are

Transmission line:

$X_{ts} = 0.3\text{p.u.}, X_{sb} = 0.3\text{p.u.}, X_s = 0.3\text{p.u.}$

Generator:

$X_d = 0.8\text{p.u.}, X_q = 0.4\text{p.u.}, X'_d = 0.2\text{p.u.},$

$M = 8\text{s.}, D = 2.35\text{p.u.}, T'_{d0} = 5\text{s.}$

AVR: $T_A = 0.01\text{s.}\, K_A = 100\text{p.u.}$

Initial load condition:

$V_t = 1.0\text{p.u.}, V_s = 1.0\text{p.u.},$

$V_b = 1.0\text{p.u.}, P_{ts} = 0.5\text{p.u.}$

3.1 Effect of ESS voltage control on the damping of power system oscillations

As it is pointed out in the previous analysis, ESS can be equipped with voltage control to regulate the voltage at the busbar where it is installed. ESS voltage control can be implemented through regulating either V_c or γ. The voltage control law can be the simple proportional control as it is assumed in the previous analysis. Figure 8 shows the small-signal simulation results (1% increase of mechanical power input at 1.0 second of simulation) of the power system without ESS voltage control. Figure 9 and 10 are the simulation result with ESS voltage control through regulating V_c ($K_{volV} = 1$)and γ ($K_{vol\gamma} = 1$) respectively. In Figure 9 and 10, the P_{ts} -δ' trajectory of movement of system operating point with ESS voltage control implemented is also presented, which confirms Figure 4 and 5.

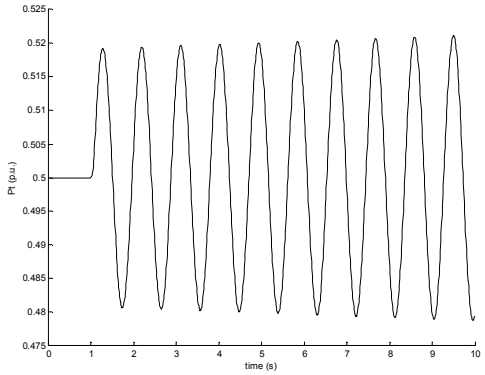

Figure 8 Small-signal simulation results without ESS voltage control

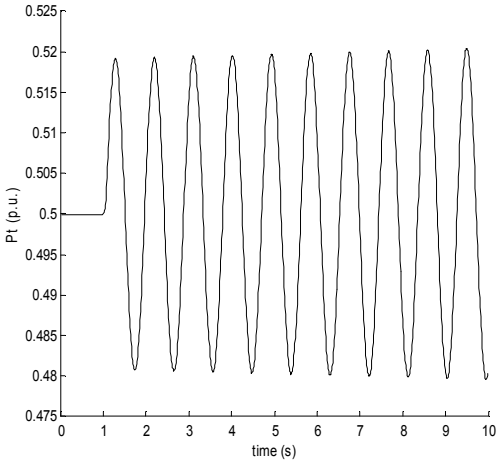

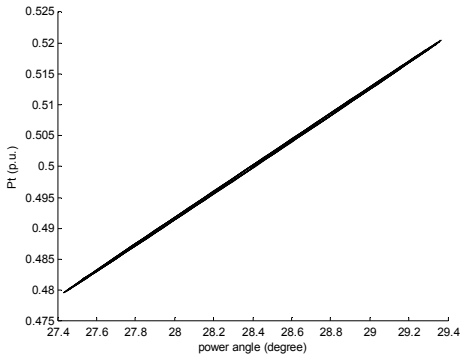

Figure 9 Small-signal simulation results with ESS voltage control implemented through regulating V_c

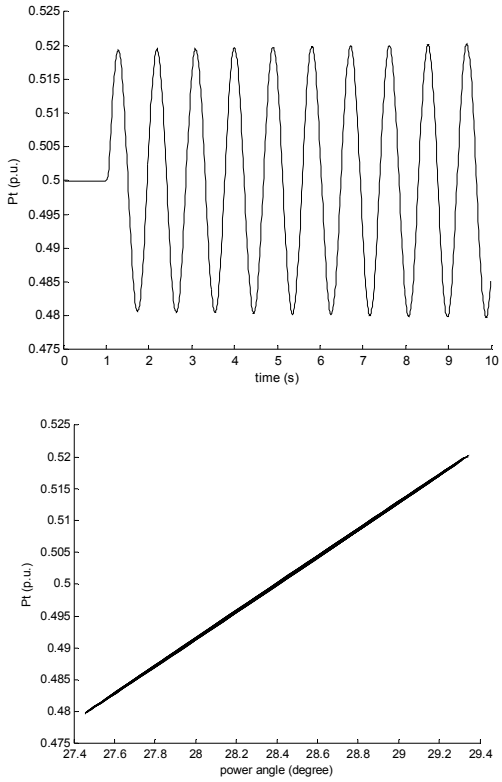

Figure 10 Small-signal simulation results with ESS voltage control implemented through regulating γ

However, a proportional control usually is not able to provide satisfactory performance of voltage regulation. Hence Figure 11 and 12 give the step-response simulation results of when the ESS voltage control is implemented by a PI controller through regulating either V_c or γ, that is, either

$$V_c = V_{c0} + (K_{volV} + \frac{K_{volVI}}{s})(V_{sref} - V_s)$$

or

$$\gamma = \gamma_0 + (K_{vol\gamma} + \frac{K_{vol\gamma I}}{s})(V_{sref} - V_s)$$

From Figure 11 we can see that when the voltage control is implemented through regulating V_c, with $K_{volV} = 1, K_{volVI} = 5$, satisfactory voltage control performance is obtained. While from Figure 12 we can see that when the voltage control is implemented through regulating γ, we can not obtain good performance of voltage regulation due to system oscillation. This is true because regulating γ leads to the exchange of active power between the ESS and power system, which does not have direct impact on the voltage regulation of the power system.

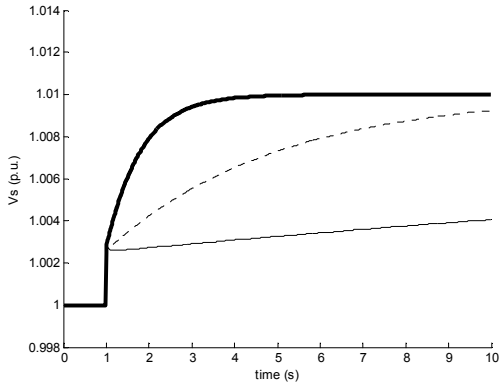

Figure 11 Step-response simulation of ESS voltage control through regulating V_c

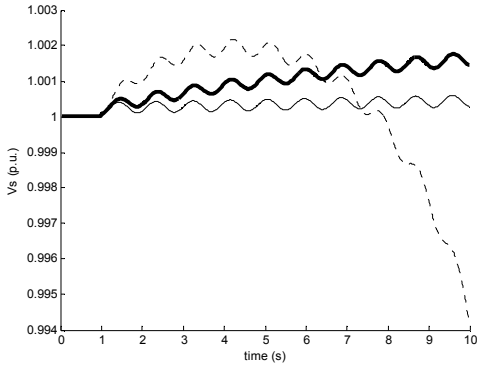

Figure 12 Step-response simulation of ESS voltage control through regulating γ

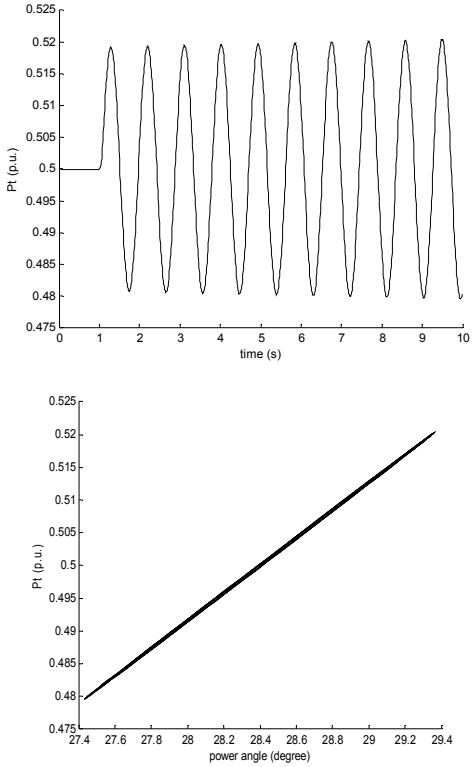

Figure 13 Small-signal simulation results with ESS voltage control implemented through regulating V_c with a PI controller ($K_{volV}=1, K_{volVI}=5$)

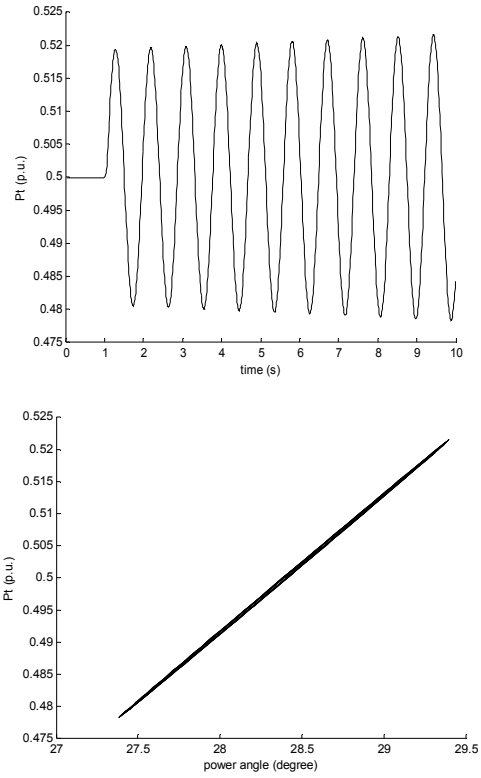

Figure 14 Small-signal simulation results with ESS voltage control implemented through regulating γ with a PI controller ($K_{vol\gamma}=1, K_{vol\gamma I}=1$)

Figure 13 and 14 present the small-signal simulation results when the ESS voltage control is implemented by a PI controller through regulating either V_c ($K_{volV}=1, K_{volVI}=5$) or γ ($K_{vol\gamma}=1, K_{vol\gamma I}=1$) and associated P_{ts} -δ' trajectory of movement of system operating point. Comparing Figure 14, 13, 10, 9 and 8 we can clearly see that the ESS voltage control has little influence on the damping of power system oscillation as it is concluded from the analysis in the above section.

3.2 ESS to damp power system oscillation

Analysis in the previous section concludes that the ESS can be equipped a damping control to improve power system oscillation by regulating either V_c or γ. It is also shown that the ESS voltage control can be implemented by regulating V_c. Hence the ESS can perform both the voltage and damping control by either superimposing the damping function on the voltage control, that is,

$$V_c = V_{c0} + (K_{volV} + \frac{K_{volIV}}{s})(V_{sref} - V_s) + K_{dampV}\Delta\omega \quad (20)$$

or by regulating γ to realize the damping function, that is,

$$V_c = V_{c0} + (K_{volV} + \frac{K_{volIV}}{s})(V_{sref} - V_s)$$
$$\gamma = \gamma_0 + K_{damp\gamma}(\omega - 1) \quad (21)$$

Figure 15 and 16 gives the small-signal simulation result and the associated P_{ts} -δ' trajectory when the ESS voltage and damping control is are implemented according to Eq.(20) ($K_{volV}=1, K_{volVI}=5, K_{dampV}=100$) and (21) ($K_{volV}=1, K_{volVI}=5, K_{damp\gamma}=20$) respectively. From it we can see that system

oscillation is well damped and especially the P_{ts} -δ' trajectory obtained confirms exactly Figure 6 and 7. This shows that the ESS damping function indeed generates an additional deviation of active power proportional to the rotor speed of the generator that results in the P_{ts} -δ' trajectory in Figure 7 confirmed by Figure 15 and 16.

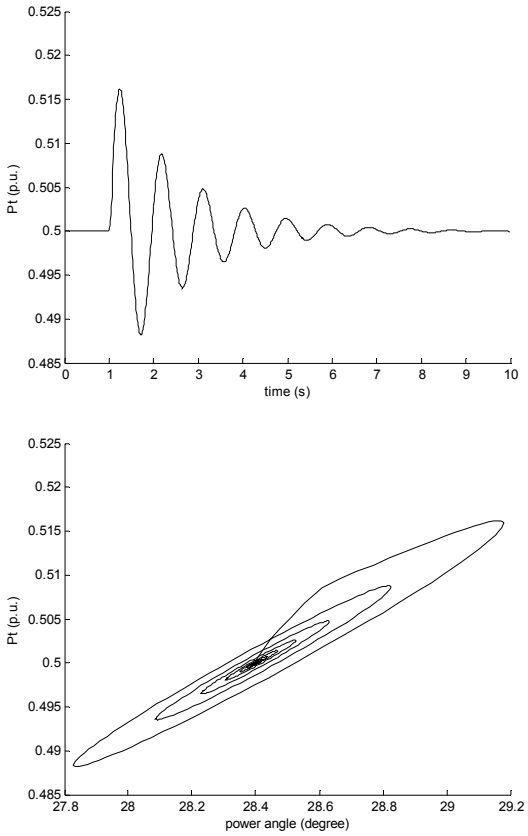

Figure 15 Small-signal simulation results with ESS damping control superimposed on ESS voltage control

$$(K_{volV} = 1, K_{volVI} = 5, K_{dampV} = 100)$$

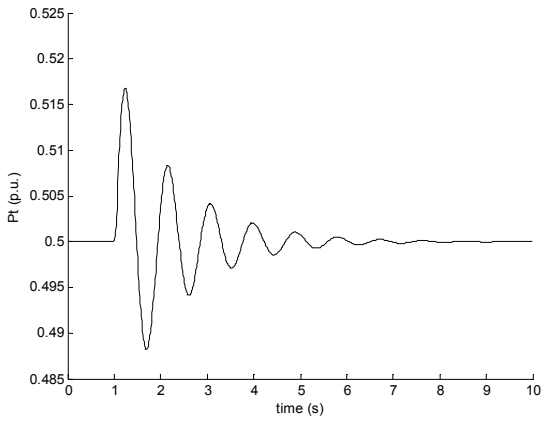

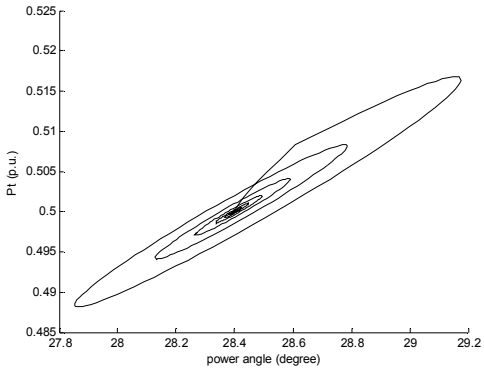

Figure 16 Small-signal simulation results with ESS damping control implemented by regulating γ

$$(K_{volV} = 1, K_{volVI} = 5, K_{damp\gamma} = 20)$$

When the damping function is superimposing on the ESS voltage control, damping control is realized by regulating V_c through the exchange of reactive power between the ESS and power system. While when it is realized through regulating γ, it directly results in the exchange of active power between the ESS and power system. Because system oscillation is the active power variation, hence regulating the active power exchange between the ESS and power system should be more effective in damping power system oscillation. Therefore, in order to compare the damping effect of regulating V_c and γ by the ESS, Figure 17 shows the small-signal simulation results when $K_{volV} = 1, K_{volVI} = 5, K_{dampV} = 20$. Comparing Figure 17 and 16 we can see that the same damping control effort implemented through regulating V_c gives less effective damping result that that achieved by regulating γ. Hence indeed, regulating the exchange of active power between the ESS and power system is more successful to suppress power system oscillation. Simulation tests are also carried out for three study cases of Figure 15, 16 and 17 when the ESS voltage control is implemented by a proportional controller.

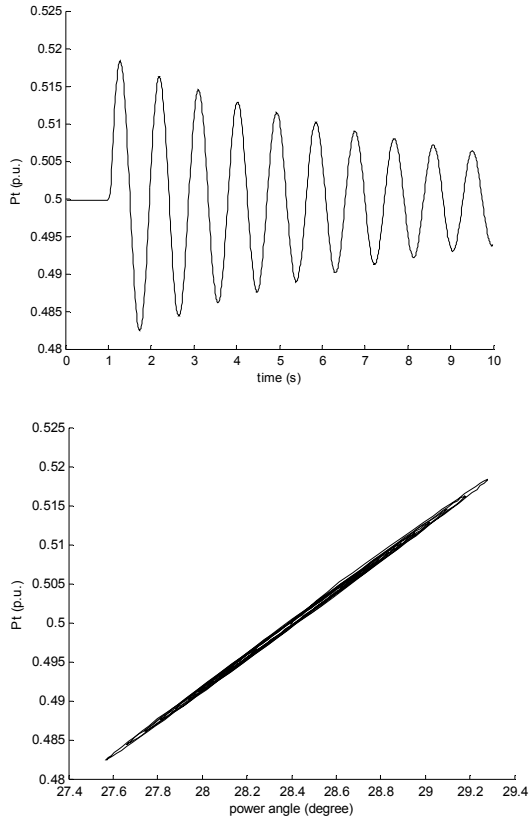

Figure 17 Regulating the exchange of reactive power between the ESS and power system is less effective in damping power system oscillation ($K_{volV}=1, K_{volVI}=5, K_{dampV}=20$)

The analysis in the previous section shows that a higher C_{Ddelta} will lead to better damping effect implemented by ESS. Hence calculation of C_{Ddelta} can give the estimation of the damping effectiveness of ESS damping controller to assess its robustness to the variation of power system operating condition. Figure 18 and 19 show the results of C_{Ddelta} calculation when the ESS damping control is implemented through regulating V_c and γ respectively. From Figure 18 we can see that when the ESS damping is through regulating V_c, the higher the load flow, the better the damping effect. Figure 18 also shows that when the ESS damping controller is implemented through regulating γ, its damping effect does not change very much, hence exhibiting better robustness to the variation of power system load condition. Confirmation of C_{Ddelta} calculation of Figure 18 by small-signal simulation is given in Figure 19-22. Figure 19 and 20 are the results of small-signal simulation results with ESS damping control superimposed on ESS voltage control when $K_{volV}=1, K_{volVI}=5, K_{dampV}=100$, $V_t=1.0\text{p.u.}, V_s=1.0\text{p.u.}, V_b=1.0\text{p.u.}$ and the power system operates at two different load conditions $P_{ts}=0.1\text{p.u.}$ and $P_{ts}=0.9\text{p.u.}$ Figure 20 and 21 are the small-signal simulation results with ESS damping control implemented by regulating γ when $K_{volV}=1, K_{volVI}=5, K_{damp\gamma}=20$ and the power system operates at two different load conditions $P_{ts}=0.1\text{p.u.}$ and $P_{ts}=0.9\text{p.u.}$, both with $V_t=1.0\text{p.u.}, V_s=1.0\text{p.u.}, V_b=1.0\text{p.u.}$

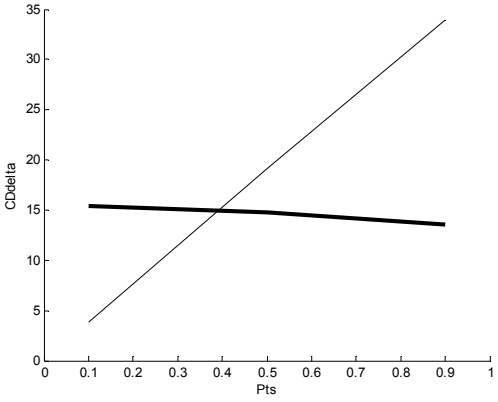

Figure 18 Results of C_{Ddelta} calculation

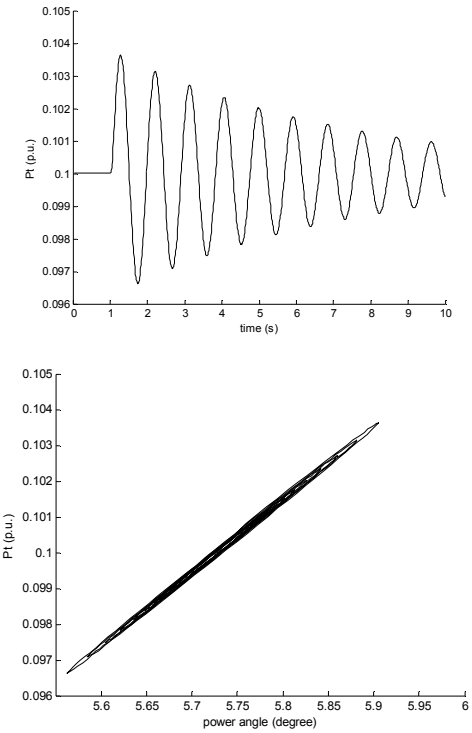

Figure 19 Small-signal simulation results with ESS damping control superimposed on ESS voltage control ($K_{volV}=1, K_{volVI}=5, K_{dampV}=100$) when $P_{ts}=0.1$p.u.

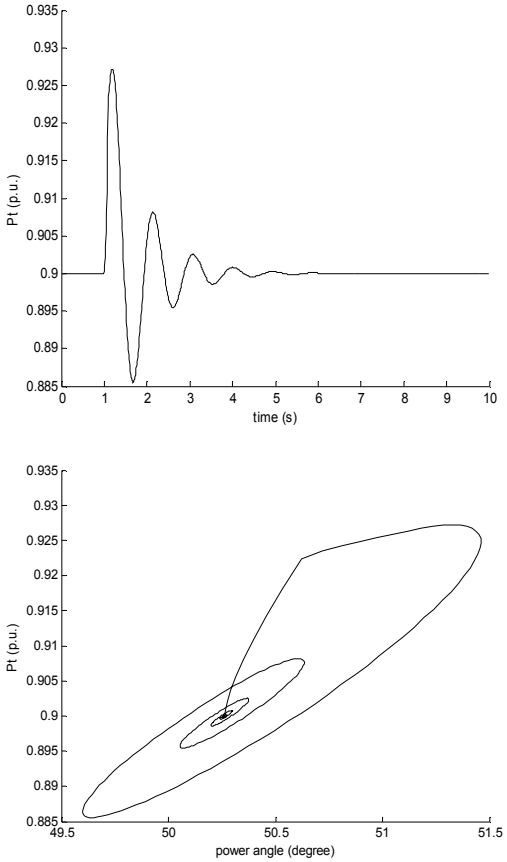

Figure 20 Small-signal simulation results with ESS damping control superimposed on ESS voltage control ($K_{volV}=1, K_{volVI}=5, K_{dampV}=100$) when $P_{ts}=0.9$p.u.

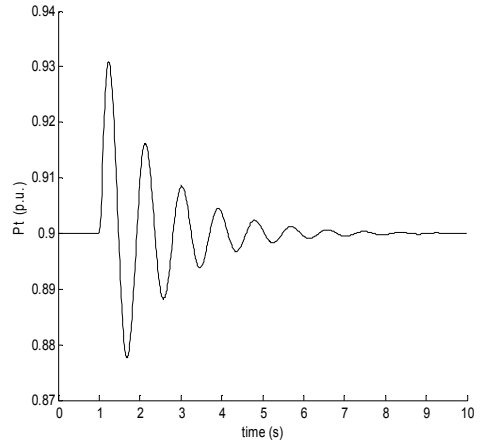

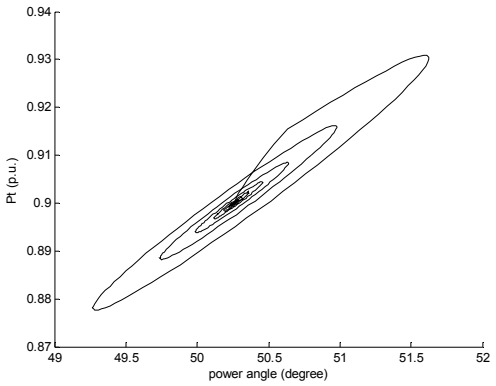

Figure 21 Small-signal simulation results with ESS damping control implemented by regulating γ ($K_{volV}=1, K_{volVI}=5, K_{damp\gamma}=20$) when $P_{ts}=0.1$p.u.

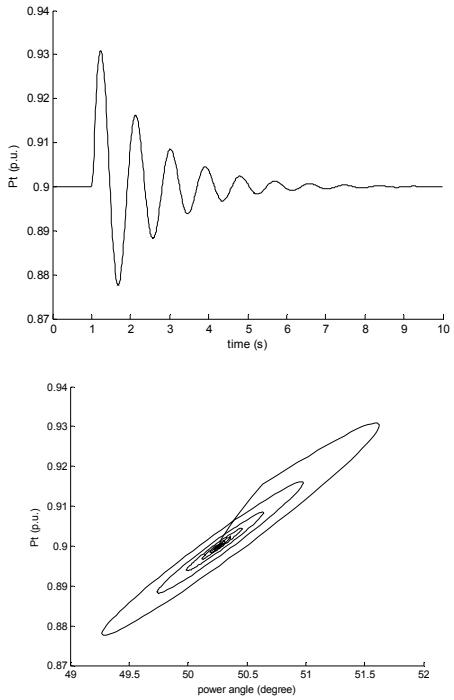

Figure 22 Small-signal simulation results with ESS damping control implemented by regulating γ ($K_{volV}=1, K_{volVI}=5, K_{damp\gamma}=20$) when $P_{ts}=0.9$p.u.

2 Example of applying BESS in damping power system oscillations

In the example power system of Figure, a BESS is installed. In this section, theoretical analysis

given in section 2 of the paper will be demonstrated through this example of power system installed with the BESS. The system parameters and initial operating condition of the example are

Transmission line:

$X_{ts} = 0.3\text{p.u.}, X_{sb} = 0.3\text{p.u.}, X_s = 0.3\text{p.u.}$

Generator:

$X_d = 0.8\text{p.u.}, X_q = 0.4\text{p.u.}, X'_d = 0.2\text{p.u.}, M = 8\text{s}.$

$D = 2.35\text{p.u.}, T'_{d0} = 5\text{s}.$

AVR: $T_A = 0.01\text{s}. K_A = 100\text{p.u.}$

Initial load condition:

$V_t = 1.0\text{p.u.}, V_s = 1.0\text{p.u.}, V_b = 1.0\text{p.u.}, P_{ts} = 0.5\text{p.u.}$

Dynamic model of the installed BESS is shown in Figure 23 [18]. Part(a) of the model is for the active power regulation along the transmission line where P_t is the line active power. Part(b) is that for the dynamic voltage support at the busbar where the BESS is installed.

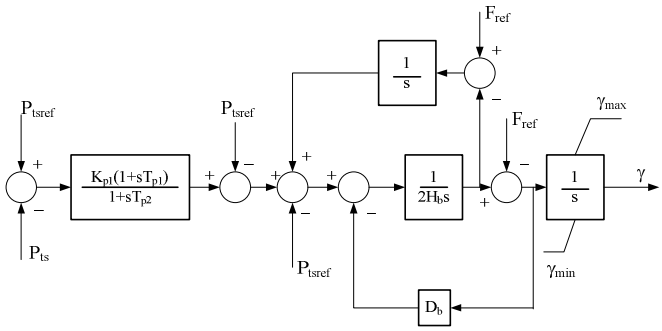

Figure 23 Dynamic model of BESS

Figure 24 shows the small-signal simulation results without and with the BESS voltage control. From it we can see that the BESS voltage control has little influence on the damping of power system oscillation. Figure 24(c) also demonstrates that exactly same trajectory of P_{ts}-δ movement as it is given in the theoretical analysis (Figure 4 and 5). In this simulation, parameters of the BESS PI voltage controllers are $K_{pvi} = 200,\ K_{pvp} = 1$.

A damping controller then is designed and superimposed on the BESS voltage controller. Figure 25 gives the small-signal simulation results that demonstrate the effectiveness of the BESS damping controller in suppressing power system oscillation. Figure 25(b) is the P_{ts}-δ trajectory that is also exactly same as it is give in Figure 6 and 7 of theoretical analysis.

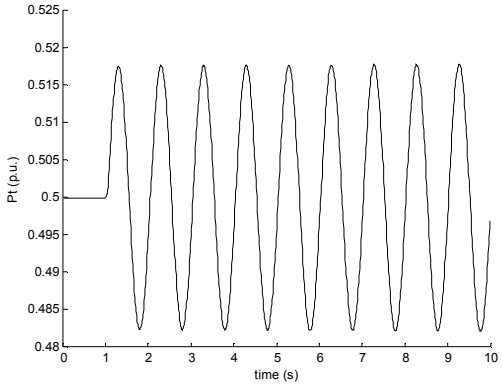

Figure 24(a) Without BESS voltage control

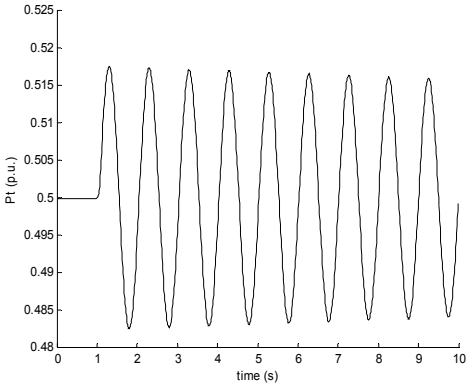

Figure 24(b) With BESS voltage control

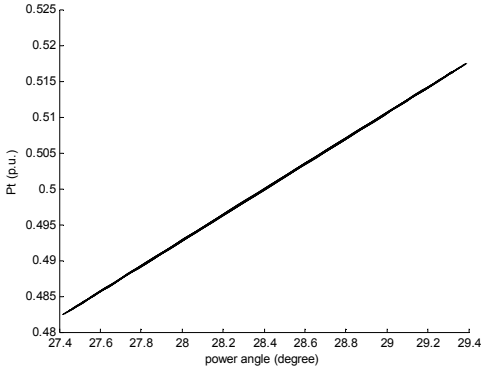

Figure 24(c) P_{ts}-δ trajectory with BESS voltage control

Figure 24 Small-signal simulation results without and with BESS voltage control

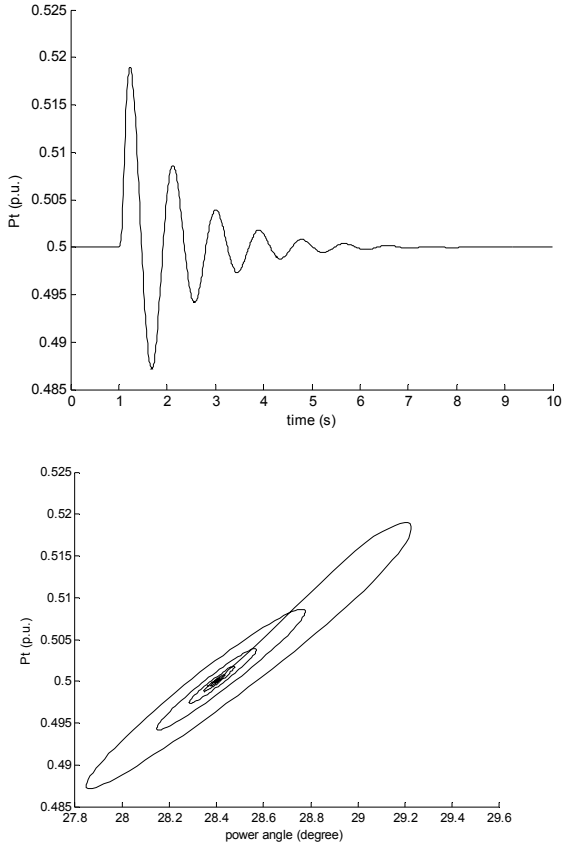

Figure 25 Small-signal simulation results with BESS damping control superimposed on its voltage control

Theoretical analysis in Eq.(18) indicates the interaction between the voltage control and damping control. When the control strength of voltage control increases with a higher gain value, damping effect of damping control measured by C_{Ddelta} will decrease. This is demonstrated by the simulation results of Figure 26 compared with those given in Figure 25. In Figure 26, gains of BESS PI voltage controller increases to be $K_{pvi} = 500, K_{pvp} = 3$ while parameters of the damping controller remain unchanged. Obviously we can see that the damping effect with higher gains of voltage controller is worse compared to that in Figure 25.

As it is pointed out in the theoretical analysis above, to suppress power system oscillation, the damping control function can also be arranged through regulating angle γ of the BESS. Figure 27 gives the small-signal simulation results when the damping control is through the regulation of angle γ while the BESS voltage controller remains unchanged as it is in Figure 24. From Figure 27 we can see that same damping effect is achieved as that given in Figure 25.

From Eq.(16) we can see that with this separation of arranging the damping control on g and the voltage control on V_c, C_{Ddelta} does not vary much with the variation of gain value of the voltage controller. Hence there should no interaction between the BESS voltage and damping control function. This conclusion of theoretical analysis is demonstrated by the small-signal simulation results of Figure 28 with higher gains of the BESS voltage controller ($K_{pvi} = 500, K_{pvp} = 3$). Comparing Figure 27 and 28 we can see that there is no influence of increasing the gains of voltage control on the effectiveness of the damping control.

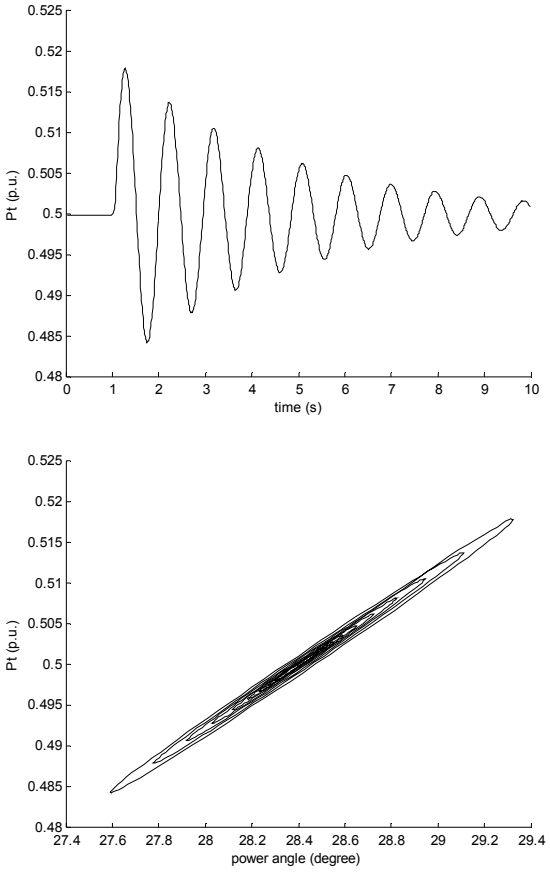

Figure 26 Small-signal simulation results with BESS damping control superimposed on its voltage controller with higher gain value

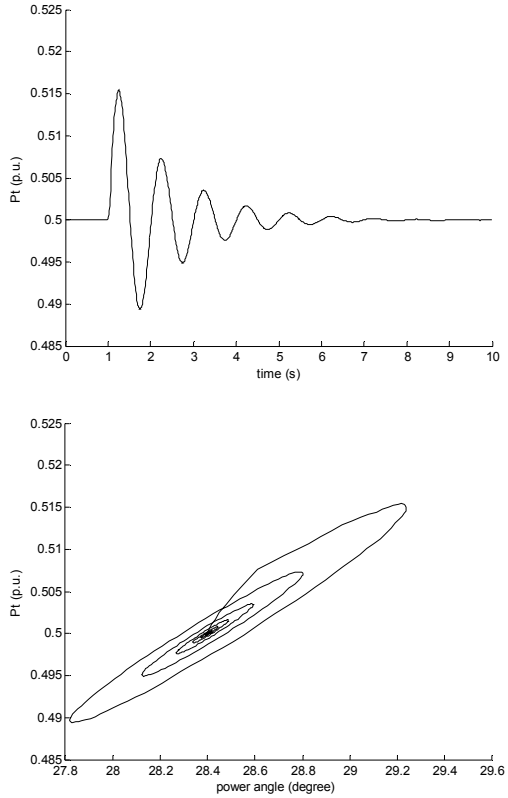

Figure 27 Small-signal simulation results with BESS damping control on g separately with its voltage control

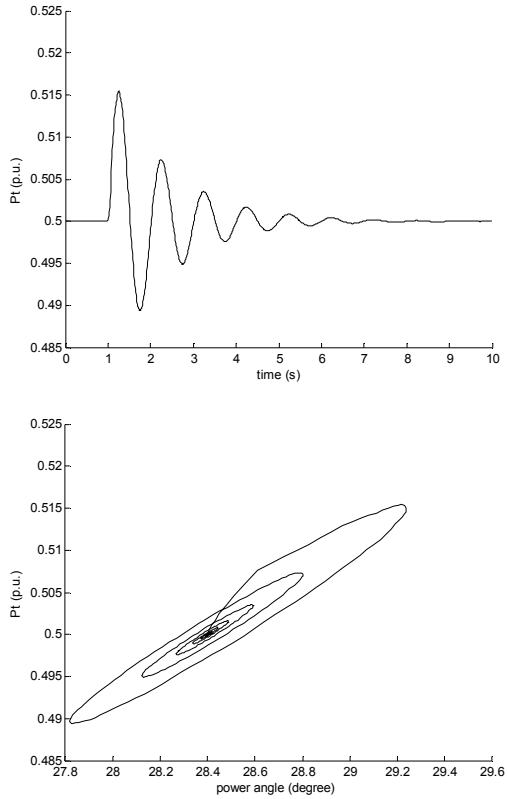

Figure 28 Small-signal simulation results with BESS damping control on γ separately and the voltage controller has higher gains

As it is pointed out in the above section that with the variation of load flow of the power system, change of effectiveness of damping control is different when it is implemented through regulating the magnitude and the phase of energy storage device. This is also confirmed by the simulation for the example power system installed with the BESS. Figure 29 and 30 are the simulation results when the damping control is superimposed on the voltage control of the BESS at two different level of load flow conditions $P_{ts} = 0.1\text{p.u.}$ and $P_{ts} = 0.9\text{p.u.}$. From Figure 29 and 30 we can see that at a higher load flow condition, the damping controller is more effective. Figure 31 and 32 show the simulation results when the damping control is implemented through regulating the angle γ. From Figure 31 and 32 we can see the effectiveness of the damping control dose not change much. Those results above are exactly same as those obtained in the above section and confirm the analytical conclusions given in section 2 of the paper. Hence we can conclude that for the damping control implemented by an ESS, better robustness of control performance can be achieved if the control is through regulating the angle γ of the ESS.

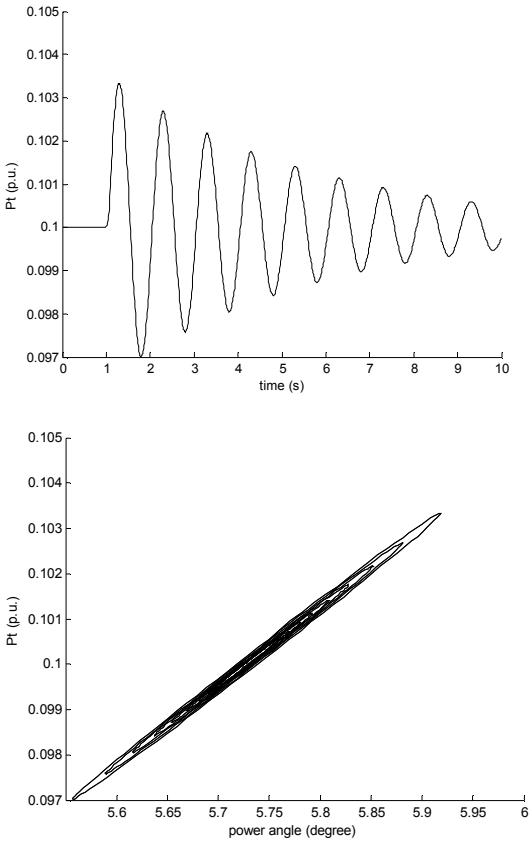

Figure 29 Small-signal simulation results with BESS damping control superimposed on the voltage control when $P_{ts} = 0.1$p.u.

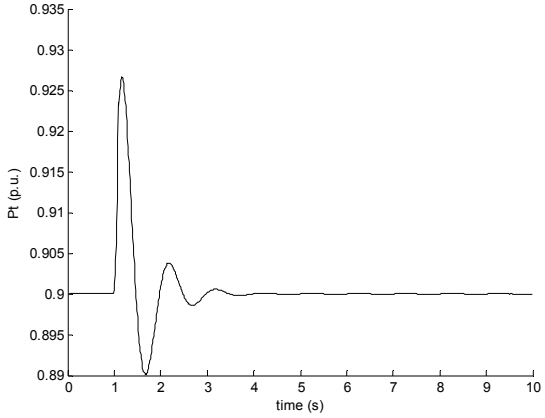

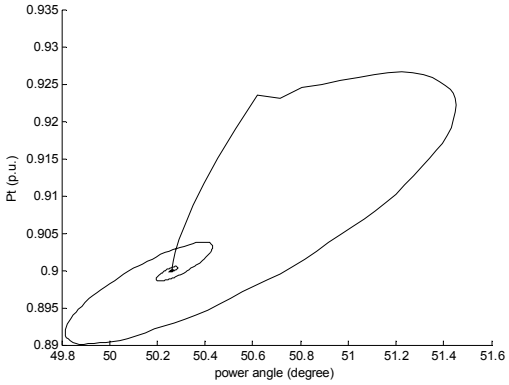

Figure 30 Small-signal simulation results with BESS damping control superimposed on the voltage control when $P_{ts} = 0.9$p.u.

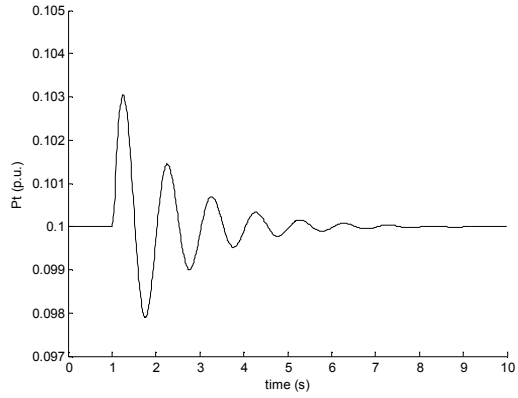

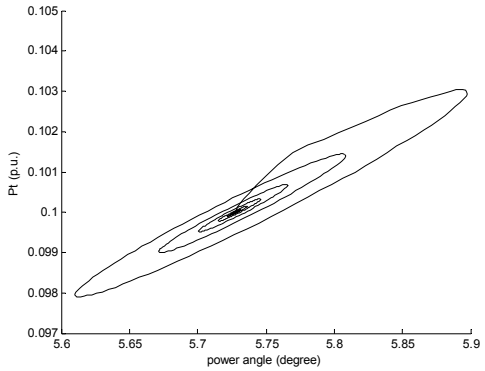

Figure 31 Small-signal simulation results with BESS damping control implemented through regulating angle γ when $P_{ts} = 0.1$p.u.

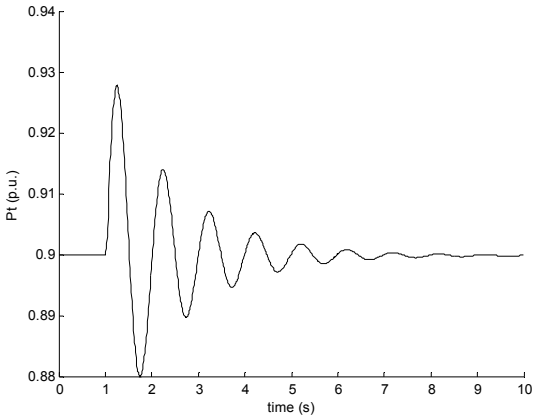

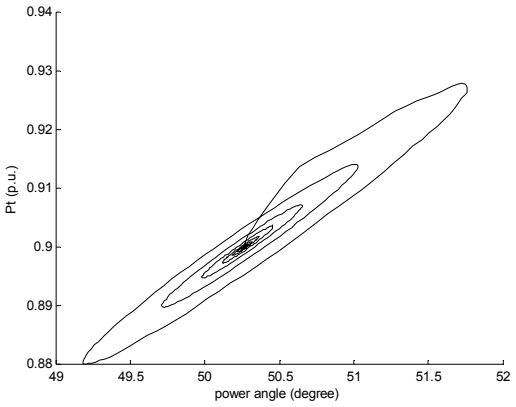

Figure 32 Small-signal simulation results with BESS damping control implemented through regulating angle γ when $P_{ts} = 0.9$p.u.

3 Extension to the case of a multi-machine power system

Without loss of generality, we assume a VSC based FACTS device is installed on the transmission line between node 1 and 2 in a

multi-machine power system as shown by Figure 13. Using the similar procedure obtained Eq.(1) we can have

$$\overline{V}_1 = jX\overline{I}_{1s} + \overline{V} \qquad (12)$$

where

$$X = (X_{1s} + \frac{X_S X_{s2}}{X_S + X_{s2}}) \quad ,$$

$$\overline{V} = \frac{X_{s2}}{X_S + X_{s2}}\overline{V}_C + \frac{X_S}{X_S + X_{s2}}\overline{V}_2 = a\overline{V}_C + b\overline{V}_2$$

Hence the active power delivered along the transmission line is

$$P = \frac{V_1 V}{X}\sin\delta'$$

where d' is the imaginary power angle between $\overline{V}_1$ and the imaginary voltage $\overline{V}$. Then the effect of the VSC based FACTS control can be considered in a similar way from Eq.(3) to (10). Same conclusion as that obtained for the single-machine infinite-bus power system can be drawn for the multi-machine power system about the damping of power oscillation on the transmission line between node 1 and 2, which can be stated as follows:

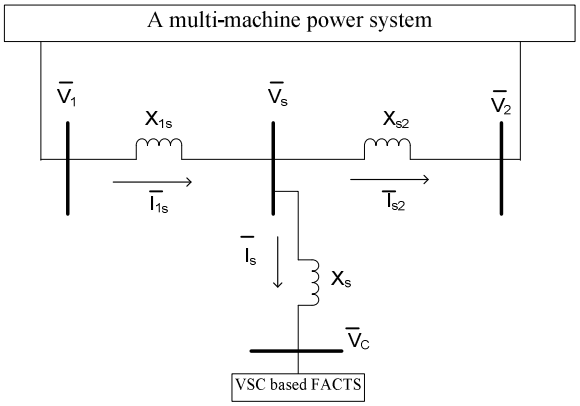

Figure 13 A multi-machine power system installed with a VSC based FACTS device

Conclusion for the multi-machine power system: for the damping of power oscillation, the VSC based FACTS control should generate a forced deviation of active power delivered along the transmission line that is proportional to the derivative of the deviation of the imaginary power angle.

Due to the limitation of space, details about the multi-machine power system will not be presented in another paper to come out soon.

4 Conclusions

Major contribution of this paper is the proposal of a general analytical method to study the damping effect of VSC based FACTS stabilizers based on the equal-area criterion. The method can be used to explain clearly and simply why and how a VSC based FACST stabilizer can suppress power system oscillation. The method can be easily extended to the case of multi-machine power systems.

References

[1] Paulo F Ribeiro, Brian K Johnson, Mariesa L Crow, Aysen Arsoy and Yilu Liu, 'Energy storage systems for advanced power applications', *Proc. of the IEEE*, Vol.89, No.12, Dec. 2001, pp1744-1756

[2] Gang Li, Shijie Chen, Jinyu Wen, Yuan Pan and Jia Ma, 'Power system stability enhancement by a double-fed induction machine with a flywheel energy storage system',

[3] M H Wang and H C Chen, 'Transient stability control of multimachine power systems using flywheel energy injection', *IEE Proc. on Generation, Transmission and Distribution*, Vol.152, No.5, 2005, pp589-596

[4] J Svensson, P Jones and P Halvarsson, 'Improved power system stability and reliability using innovative energy storage technologies',

[5] L Zhang, C Chen M L Crow and S Atcitty, 'Comparision of FACTS integrated with battery energy storage systems',

[6] W R Lachs and D Sutanto, 'Application of battery energy storage in power systems',

[7] Bharat Bhargava and Gary Dishaw, 'Application of an energy source power system stabilizer on the 10MW battery energy storage system at Chino substation', *IEEE Transaction on Power Systems*, Vol.13, No.1, 1998, pp

[8] Satish Samineni, Brian K Johnson, Herbert L Hess and Joseph D Law, 'Modelling and analysis of a flywheel energy storage system for voltage sag correction', *IEEE Transaction on Industry Applications*, Vol.42, No.1, 2006

[9] Toshifumi Ise, Masanori Kita and Akira Taguchi, 'A hybrid energy storage with a SMES and secondary battery', *IEEE Transaction on Applied Superconductivity*
[10] S Arabi and P Kundur, 'Stability modelling of storage devices in FACTS applications',

Acknowledgements
The authors would like to acknowledge the support of the EPSRC Supergen 3 – Energy Storage Consortium, UK, the National Natural Science Foundation of China (No.50577007) and the Power System Stability Study Institute, NARI Group, China

[3] E.V.Larsen, J.J.Sanchez-Gasca and J.H.Chow, "Concept for design of FACTS controllers to damp power swings", IEEE T-PWRS, Vol.10, 1995
[4] M. Noroozian and G.Andersson, "Damping of Power System Oscillations by use of Controllable Components", IEEE T-PD, Vol.9,1994
[5] H.F.Wang and F.J.Swift, 'The capability of the Static Var Compensator in damping power system oscillations', *IEE Proc. Part C,* May, No.4, 1996
[6] F.J.Swift and H.F.Wang, 'The Connection Between Modal Analysis and Electric Torque Analysis in Studying the Oscillation Stability of Multi-machine Power Systems', *Int. Journal of Electrical Power and Energy Systems*, No.5, 1996